Materials and Structures/Matériaux et Constructions, Vol. 31, May 1998, pp 218-224

SCIENTIFIC REPORTS

Determination of moisture distributions in porous building materials by neutron transmission analysis

H. Pleinert[1], H. Sadouki[2] and F.H. Wittmann[2]

(1) Paul Scherrer Institute, Villigen, Switzerland

(2) Swiss Federal Institute of Technology, Zurich, Switzerland

Paper received: January 28, 1997; Paper accepted: February 28, 1997

ABSTRACT

The movement of moisture inside building structures can affect them in important ways, causing physical and chemical damage. Therefore the study of moisture transport in porous building materials is highly relevant to a better understanding of the durability of building structures made of porous materials. The moisture transport can be described phenomenologically by a diffusion equation using a moisture content dependent moisture transfer coefficient. To determine the transfer coefficient in a given material, the experimental quantitative measurement of the time and space dependent moisture distribution in the material is necessary. Neutron radiography provides a highly sensitive non-destructive method for the detection of the presence of water and provides high spatial resolution. A new neutron transmission analysis technique has been developed and optimized for the study of moisture in building materials to extract the quantitative information from the experimental data. Typically, moisture contents down to a few mg/cm^3 can be detected at a spatial resolution of 1 mm. As an application example, the determination of the time and space dependent moisture distribution in a brick sample and the subsequent determination of the moisture transfer coefficient are presented.

RÉSUMÉ

Les mouvements d'eau au sein de la structure poreuse d'un ouvrage peuvent l'affecter sérieusement, notamment par une dégradation physique ou chimique. Aussi est-il nécessaire de bien comprendre les mécanismes de transfert d'humidité pour une meilleure maîtrise des problèmes liés à la durabilité des constructions en matériaux poreux. Les transferts d'humidité sont souvent décrits d'une façon phénoménologique, par des équations de type diffusion, mettant en jeu un ou plusieurs coefficients de transfert. Une méthode de détermination des coefficients de transfert hydrique d'un matériau consiste à les extraire de l'information contenue dans les distributions spatio-temporelles de teneur en eau mesurées. La radiographie à neutrons s'avère être une technique de mesure non-destructive de très grande sensibilité pour détecter la présence d'eau, avec notamment une haute résolution spatiale. Une nouvelle technique d'analyse de la transmission neutronique a été développée et optimisée pour l'étude d'analyses hydriques des matériaux poreux, permettant d'extraire des informations quantitatives à partir des données expérimentales. Typiquement, des humidités inférieures à quelques mg/cm^3 peuvent être détectées avec une résolution spatiale de 1 mm. À titre d'exemple d'application, nous avons déterminé les distributions spatiales d'humidité, à différents temps de dessiccation, dans un échantillon de brique, puis nous avons déduit le coefficient de transfert hydrique du matériau.

1. INTRODUCTION

The penetration of moisture into building structures can cause damage by the action of chemical contaminant agents transported by the water, by the action of microorganisms growing in the humid environment or by the mechanical action of freezing and thawing. On the other hand, most of the penetrating water later leaves the porous system by drying, which can cause shrinkage and carbonation in cementitous materials. As many building materials are porous, the understanding of moisture transport in the porous system represents an important issue in building technology.

Several transport mechanisms of liquid water and water vapor contribute to the movement of moisture in the porous system. Their action is usually described by a diffusion model that combines them into a single moisture diffusivity described by a non-linear diffusion equation governed by a moisture content dependent transfer coefficient. For a given material, this coefficient has to

Editorial note

Prof. Dr. Folker H. Wittmann is a RILEM Senior Member. He is the outgoing President of the Association and a member of the Bureau. He participates in the work of the editorial group of TC 90-FMA (Fracture Mechanics of Concrete - Applications) and the activities of TC 107-CSP (Creep and Shrinkage Prediction Models).

be determined from experimental data of moisture distributions inside samples of the material under defined starting and boundary conditions.

To effectuate this measurement, a non-destructive technique sensitive to the presence of water and providing information on the spatial distribution of the moisture is required. Several suitable non-destructive-methods exist for measuring the moisture distribution inside a sample and providing spatial resolution in the range of 1 mm or less. They can be subdivided into two groups: NMR methods [1] based on electromagnetic interaction with the water in the porous system, and radiography methods based on weakening of radiation passing through matter, using X-rays [2], γ-rays [3] or neutrons [4] to visualize the contrast between regions containing different amounts of moisture. NMR methods can distinguish between free, physically bound and chemically bound water, but interference may be caused by the presence of paramagnetic ions in most building materials. Radiography methods do not differentiate between free and bound water, but are not subject to electromagnetic interference and may offer higher spatial resolution, depending on the source quality. Among the radiography methods, neutron radiography offers the highest hydrogen detection sensitivity.

Neutron radiography can be performed either as scanning neutron radiography [5] with monochromatic neutrons and a small beam cross-section, or as direct neutron radiography [6] using a thermal or cold non-monochromatic neutron beam. In scanning neutron radiography, effects due to scattered neutrons are minimized, making a fast and good first-order approximation evaluation possible, but the experimental procedure is complicated by the necessity of scanning along the dimensions of the sample which exceed the beam cross-section, while direct neutron radiography permits the recording of the total information in one measurement. However, in each case a basic understanding of the processes involved in the neutron transmission is necessary for a correct formulation of evaluation technique and error analysis. Several analytical methods of neutron transmission analysis exist, using signal transfer functions [7, 8] and Monte Carlo calculations. On the basis of some of the existing concepts and additionally incorporating aspects particular to the determination of moisture profiles in building material samples, it has been undertaken to design a transmission analysis technique optimized for this type of measurement [9].

This paper describes the experimental method, the preparation of samples adapted for the neutron radiographic measurement and the neutron transmission analysis technique which has been developed for the determination of moisture profiles from which the hygral diffusion coefficients are then deduced. The experimental and analytic process are illustrated by an application example describing the drying of a brick sample.

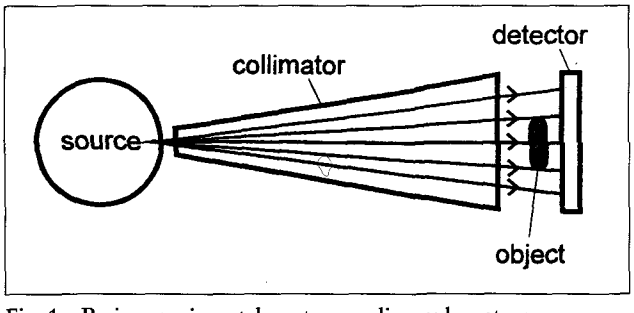

Fig. 1 – Basic experimental neutron-radiography set-up.

2. EXPERIMENTAL TECHNIQUE

2.1. Neutron radiography

The principle of radiography in general is the recording of the radiation passing through an object by a position sensitive detector. The basic experimental set-up is displayed in Fig. 1. The radiography detector records an image which is a projection of the object on the detector plane and which contains spatial information on the intensity of the radiation reaching the detector. Because the attenuation of the radiation in the object depends on material thickness and density, the image contains qualitative and quantitative information on the structure and composition of the object. Also, since the image is the projection of the three dimensional object in two dimensions, the information is averaged over the thickness of the object along the beam path.

In the case of neutron radiography, the attenuation of the beam is due to the interaction of neutrons with the nuclei of the atoms in the object material, which can occur either by scattering or absorption. The degree of attenuation of a neutron beam by a given chemical element contained in the object material is described on the macroscopic level by the macroscopic neutron cross-section $\Sigma(E)$ of that element, which is the sum of its macroscopic absorption and scattering cross-sections. The total cross-section of a material containing several chemical elements is the sum of the partial cross-sections of the N elements contained in it weighted by their mass fractions m_i:

$$\Sigma(E) = \sum_{i}^{N} m_i \Sigma_i(E) \qquad (1)$$

It follows that the total cross-section of a porous material containing an unknown quantity of moisture is a linear function of the moisture content. The macroscopic cross-section of water and typical macroscopic cross-sections for dry brick and concrete are shown in Fig. 2. The total cross-sections of brick and concrete containing moisture as functions of the moisture content are displayed in Fig. 3a and Fig. 3c. It can be seen that the cross-section of water is much larger than those of the building materials and therefore the presence of water can be detected with high sensitivity by neutron radiography.

The experimental set-up consists of a neutron source, a collimator, the object and a detector. The source can be a isotopic neutron source, an accelerator, a research reactor or a spallation source [10, 11]. Isotopic and accelerator based sources are mobile but achieve less spatial resolution than reactors or spallation sources which provide a higher beam intensity. The collimator is a beam-forming assembly, which defines the geometric properties of the beam

[12] and generally also contains filters to influence the energy spectrum of the beam and to reduce beam pollution by γ-rays. Several detector types for neutron radiography are available, the most common being X-ray or nitrocellulose film combined with suitable converter foils [13] using a scanner to digitize the recorded information, or electronic detectors which directly record digital images, consisting either of a scintillator screen and a CCD-camera [14] or of neutron sensitive imaging plates read out by a laser scanner [15].

The measurements performed for the development and verification of the technique presented in this paper have been performed at a reactor-based facility at the Atominstitute of the Austrian Universities [16] using the direct neutron radiography technique. Two detectors have been employed: a system of X-ray film with a Gd-converter foil and an electronic detector consisting of a scintillator screen and a CCD-camera cooled with liquid nitrogen. X-ray film combined with a Gd-foil presents the advantages of high spatial resolution down to 30 μm and of low cost, but a sophisticated calibration technique [17] has to be employed to achieve good reproducibility of the measurement, and the data has to be digitized after the measurement with a scanner. The CCD-camera is limited to a maximum resolution on the order of 200 mm, but permits direct recording of digital images with a high dynamic range of up to 16 bit, and the cooling by liquid nitrogen ensures high sensitivity, excellent reproducibility and negligible dark current. The principles of the two detector systems are outlined in Figs. 4a and 4b.

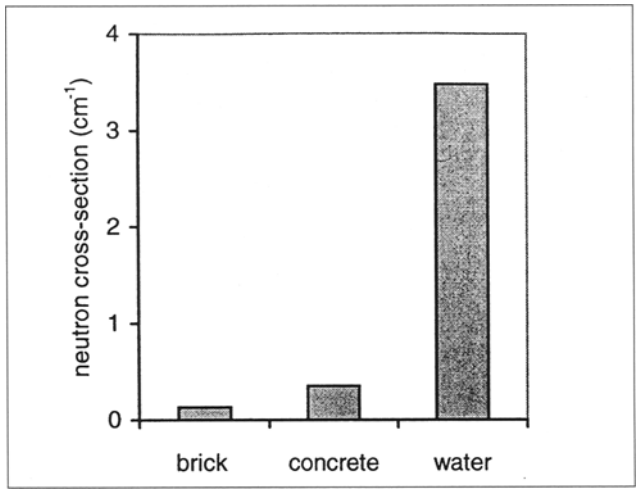

Fig. 2 – Comparison of the macroscopic neutron cross-section of water and of typical cross-sections for dry brick and concrete.

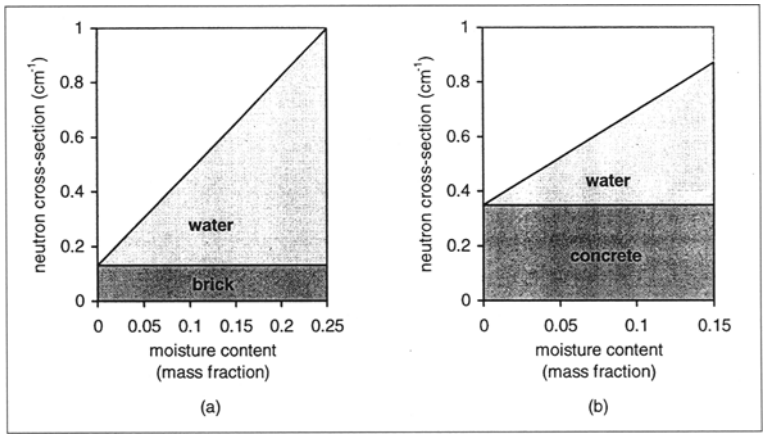

Fig. 3 – Total macroscopic neutron cross-sections of brick containing humidity (a) and concrete containing humidity as functions of the humidity content.

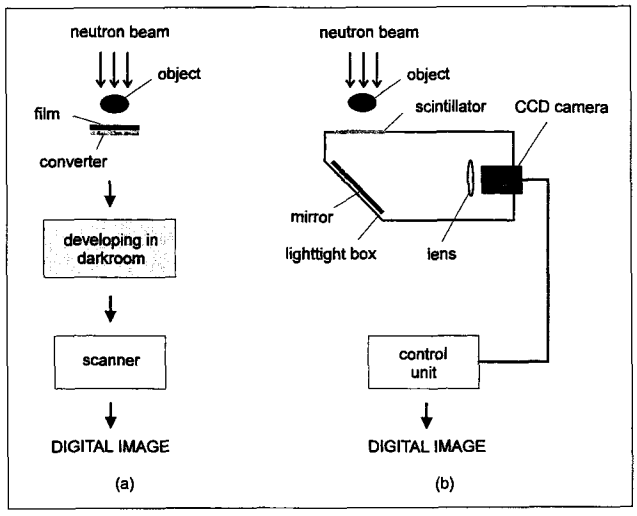

Fig. 4 – Principle of a neutron radiography detector consisting of X-ray film and a converter foil (a) and of an electronic neutron radiography detector using a cooled CCD-camera (b).

2.2. Preparation of samples

The samples are designed for the best possible yield of information by the measurement, taking into account the specific properties of the experimental method. From the nature of radiography as a method of imaging the projection of the sample, it follows that the sample should preferably be of constant thickness along the beam path. This thickness should be optimized to obtain the highest possible contrast between different amounts of moisture contained in the porous system. The optimal thickness for a given material depends on the chemical composition and density of that material and is typically in the range of 3 cm for many building materials. Geometric boundary conditions which ensure a moisture distribution that does not depend on the coordinate along the beam path should be established. This can be done by insulating all surfaces of the sample which are orthogonal to the beam path. The insulation should not contain large amounts of material which interacts strongly with neutrons, *i.e.* an insulation material with minimal or no content in hydrogen should be selected.

Taking into account these conditions, the following design has been adopted for the samples used for the measurements: a rectangular prismatic shape of dimensions 3 cm, 9 cm and 12 cm, sealed on all the 9×12 cm^2 and 9×3 cm^2 surfaces, and on either none or one of the 12×3 cm^2 surfaces. This way the moisture exchange with the outside always results in a moisture distribution which does not depend on the coordinate along the 3 cm thickness of the sample. Self-adhesive aluminum tape has been used as insulation material.

3. CALCULATION PROCEDURE

3.1. Determination of moisture distributions

The intensity of the signal recorded at a given point in the detector plane decreases with increasing moisture at the corresponding coordinates in the sample. To determine the space dependent moisture content, a relation between the recorded signal intensity and the moisture content has to established. For this, the contribution of the involved mechanisms of neutron transmission to the detector signal have to be described adequately.

Neutrons that penetrate into the sample are either transmitted without interaction, or absorbed or scattered one or several times by nuclei in the sample. It follows that two neutron flux components reach the detector: an uncollided component consisting of neutrons transmitted without interaction, and a collided component consisting of those scattered neutrons that reach the detector. The uncollided component can be described by the law of exponential weakening of radiation passing through matter [18], and in the case of sample materials with scattering cross-sections much smaller than absorption cross-sections, it can be considered a good approximation. However, it has been shown that it would constitute a poor approximation for materials consisting of elements with high scattering cross-sections and low absorption cross-sections, which generally is the case for building materials and the moisture contained in the porous system [19]. Therefore a calculation technique taking into account a strong collided flux contribution and optimized for the determination of moisture distributions in building material samples has been developed.

The technique is based on a conceptual model which describes the neutron transmission as a signal transfer process. Two sets of data are considered: the detector signal caused by the beam transmitted through the sample (**A**) and the detector signal caused by the unmodified beam in the absence of a sample (**B**). **A** can be viewed as the result of the transformation of **B** by its transfer through the system consisting of the sample, and a relation between these two signals is established using signal transfer functions. Thereby the signal generation can be described adequately without the need of explicitly taking into account the complex physical process of neutron transmission through the sample.

The transfer is described separately for the signal generated by the uncollided and the collided neutrons. Both signals are described as functions of the coordinates (x,y) in the detector plane. The beam is assumed to be parallel, which is a good approximation for the selected type of experimental facility. The detector signal **A** is considered the sum of a signal $S_{AU}(x,y)$ caused by the uncollided flux and a signal $S_{AC}(x,y)$ caused by the collided flux transmitted through the sample:

$$S_A(x,y) = S_{AU}(x,y) + S_{AC}(x,y) \tag{2}$$

The signal **B** is also considered a function $S_B(x,y)$ in the detector plane, and both components of **A** are described as the result of the action of signal transfer functions on **B**.

For the uncollided component, the transfer is a point process: the flux penetrating the sample at a given point reaches the detector at the coordinates (x,y) of the projection of that point in the detector plane, and does not contribute to the detector signal at any other point. The transfer can be described by an attenuation function $UNC(x,y)$ for the uncollided component:

$$S_{AU}(x,y) = UNC(x,y) \cdot S_{AB}(x,y) \tag{3}$$

The transfer of the collided component is a neighborhood process: the flux entering the sample at a given point with the coordinates (x',y') contributes not only to the detector signal at (x',y') but also at many other points at coordinates (x,y). The appropriate signal transfer function is a point spread function $PSF(x,y,x',y')$:

$$S_{AC}(x,y) = \int PSF(x,y,x',y') S_B(x',y') dx'dy' \tag{4}$$

On the basis of this model, the moisture distribution can be determined from the detector signal by the following calculation procedure:

- Step I - determination of the parameters of the experimental facility, *i.e.* the energy spectrum and spatial distribution of the beam and energy dependence of the detector response. The characteristics of the beam can be determined by particle transport calculations, and the detector response can be evaluated from the energy dependence of the reaction on which the detecting process is based.
- Step II - determination of the system transfer functions *UNC* and *PSF* for the given geometry and composition of the samples and geometry of relative positions of sample and detector: this step can also be performed by particle transport calculations. The detector plane is discretized into square pixels and *UNC* and *PSF* become functions of discrete coordinates (x_i,y_j). For the given characteristics of the sample, UNC and PSF depend only on the moisture $h(x_i,y_j)$ in the section of the sample which is projected on the pixel (x_i,y_j).
- Step III: evaluation of the individual measurement: because the signal transfer functions obtained in step II depend only on the moisture, the moisture distribution can now be determined by iteration. A first-order estimate $h^1(x_i,y_j)$ of the moisture distribution is derived from the observed signal $S_A(x_i,y_j)$, then the signal $S_A{}^1(x_i,y_j)$ corresponding to $h^1(xx_i,y_j)$ is calculated with the help of *UNC* and *PSF* and is compared to $S_A(x_i,y_j)$. From this a second estimation $h^2(x_i,y_j)$ is derived; the process is repeated until $S_A{}^n(x_i,y_j)$ corresponding to $h^n(x_i,y_j)$ equals the measured $S_A(x_i,y_j)$ within the precision of the measurement, and the moisture distribution is determined as $h(x_i,y_j) = h^n(x_i,y_j)$.

In general, step I and II will be performed only before beginning a series of experiments at a new experimental facility or with a new type of sample. For the measurements performed for the development and verification of the technique presented in this paper, the Monte Carlo Method [20] has been used for the particle transport calculations which have been carried out with the Monte Carlo Code MCNP [21]. Once the results of step I and step II have been obtained, only step III has to be carried out for

the individual measurements. The iteration algorithm of step III has been programmed in Visual Basic.

By repeating the procedure of step III with data from measurements recorded at different times on the same sample, a set of moisture profiles describing the time depended evolution of the moisture distribution can be obtained.

The precision at which $h(x,y)$ can be obtained depends on the chemical composition of the sample, on the moisture content and on the spatial resolution. It decreases with increasing spatial resolution, and for this reason it is practical to digitize the images at a spatial resolution in the range of 1 mm, even though the detector technology could achieve a far better resolution. For building materials, the detection limit of moisture differences is typically in the range of a few mg·cm^{-3} at a spatial resolution of 1 mm.

3.2. Determination of the moisture transfer coefficient

3.2.1. General remarks

Phenomenologically, the transient moisture flow through the porous structure of building materials such as bricks can be described by the following partial differential equation [22-24]:

$$\frac{\partial w}{\partial t} = di\left(D(w)gradw\right) \tag{5}$$

where w is the moisture content (gas and liquid phases) per volume unit of the porous material, and $D(w)$ is the global moisture-dependent transfer coefficient describing all the different mechanisms of moisture motion in the porous structure. In building materials such as bricks, capillary pressure and molecular diffusion can be regarded as the dominant mechanisms.

In case of our study, moisture transfer between the material and the surrounding atmosphere of relative humidity h_{ext} can be described by the following equation [22-24]:

$$J = A\beta(h_s(w) - h_{ext}) \tag{6}$$

where J is the moisture flux between the porous material and the outside atmosphere through the exposed surface A, β is the moisture transfer coefficient at the surface and $h_s(w)$ is the humidity concentration at the exposed surface. $h_s(w)$ is given by the desorption isotherm of the material, which is displayed in Fig. 5 [25]. At high moisture content J is constant and given by the evaporation rate.

In the above description, the temperature influence is neglected.

3.2.2. Numerical analysis

In the numerical analysis, equation (5) is used in its integral formulation [26]. We can spatially integrate equation (5) over a conveniently small finite volume V of the flow region and write:

$$\frac{\partial}{\partial t}\int wd = \int di\left(D(w)gradw\right)d \tag{7}$$

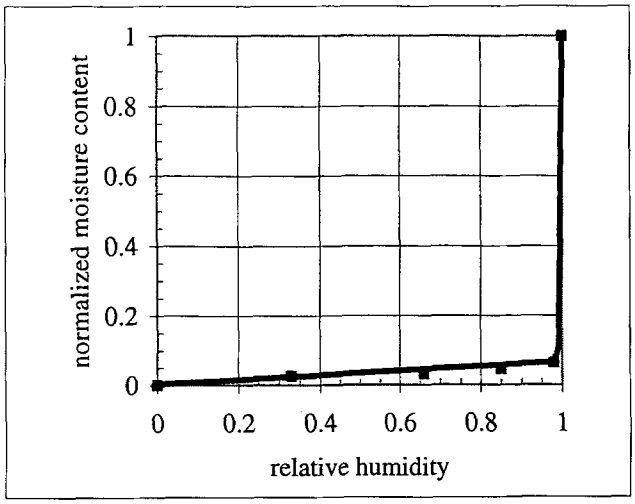

Fig. 5 – Desorption isotherm curve of a brick at 20° C, after Weimann [22].

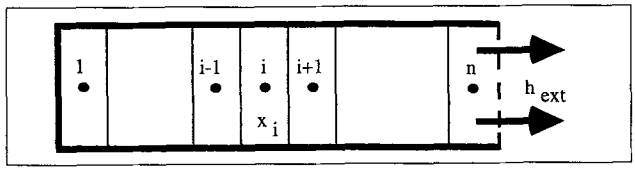

Fig. 6 – Discretization of the drying prismatic sample (sealed surfaces are in bold).

By means of the divergence theorem, the right-hand term of equation (7) is converted to a surface integral, and assuming an average value of w over V, equation (7) can be written as follows:

$$V\frac{\partial w}{\partial t} = \int_{\Gamma} D(w)gradw \cdot dA \tag{8}$$

In case of a drying prismatic specimen with five sealed faces, the flow problem is simplified to an one-dimensional one. The integrated finite difference method [26] is used to solve the problem. The flow domain is discretized into n small subdomains as shown in Fig. 6.

For the i-th element, exchanging moisture with elements $(i\text{-}1)$ and $(i+1)$, the mass balance (equation (8)) can be approximated as follows:

$$V_i\frac{\Delta w_i}{\Delta t} = D_{i-1,i}\frac{w_i - w_{i-1}}{x_i - x_{i-1}}A + D_{i+1,i}\frac{w_i - w_{i+1}}{x_i - x_{i+1}}A \tag{9}$$

For the boundary element (n), connected with the $(n\text{-}1)$-th element and the surroundings, the approximated mass balance (equations (6) and (8)) can be written as:

$$V_n\frac{\Delta w_n}{\Delta t} = D_{n-1,i}\frac{w_n - w_{n-1}}{x_n - x_{n-1}}A + \beta A\left(h_s(w) - h_{ext}\right) \tag{10}$$

In equations (9) and (10), $D_{l,k}$ is the harmonic mean transfer coefficient of the adjacent elements l and k [26].

The set of equations (5) and (10), can then be solved numerically by an adequate numerical method for the unknown w_i.

3.2.3. Determination of the material parameters

The parameter β of equation (6) is estimated by the measured rate of moisture loss (deduced from the moisture profile after 1 day of exposure to the surrounding atmosphere).

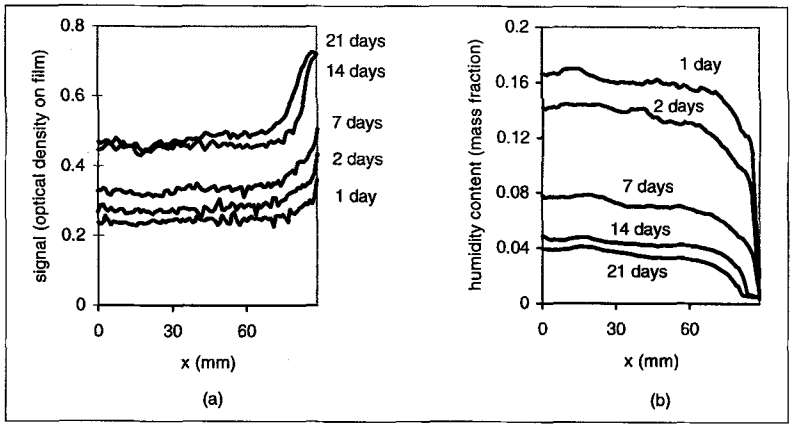

Fig. 7 – Neutron transmission profiles along the width of the sample at times t = 1, 2, 7, 14 and 21 days (a) and the corresponding humidity distributions calculated by signal transfer analysis (b).

It is assumed that the unknown moisture transfer coefficient $D(w)$ can be described by a polynome of third order (other mathematical functions can be used):

$$D(w) = D_1 + D_2 w + D_3 w^2 + D_4 w^3 \qquad (11)$$

where D_i (i = 1,4) are constant parameters to be estimated from the experimental moisture profiles.

The best parameters D_i can be obtained by comparing the calculated moisture profiles with the experimental data, and looking for the best fit. This can be realized by minimizing the functional quadratic error [27]:

$$S(P) = \sum_i \sum_j \left(w_c(t_i, x_j) - w_e(t_i, x_j) \right)^2 \qquad (12)$$

$P = (D_1,..,D_4)$ in equation (12) is the parameter vector of the transfer coefficient of equation (11), $w_c(t_i,x_j)$ is the calculated moisture content at drying time t_i and depth x_j and $w_e(t_i,x_j)$ is the measured moisture content at drying time t_i and depth x_j.

4. APPLICATION EXAMPLE

4.1. Experimental profiles

The time and space dependent moisture distribution in a drying brick sample has been determined. The sample dimensions are 12 × 9 × 3 cm³. The porous system of the sample was initially saturated with water by storing it under water. Then the sample was taken out of the water and sealed with self-adhesive aluminum tape on all sides except on one of the 3 × 12 cm² surfaces and was placed in an atmosphere of 64% relative moisture. To observe different stages of drying, radiographic images of the sample were produced at times t = 1, 2, 7, 14 and 21 days, using X-ray film and a Gd-converter. The images were digitized by a scanner to obtain $S_A(x_i,y_j)$ in an orthonormal coordinate system where the x-axis is parallel to the direction defined by the 9 cm edges of the sample, and where unity corresponds to 1 mm. Since the geometric boundary conditions permit drying only through one surface, moisture profiles depending only on x can be expected in this coordinate system. Slices of $S_A(x_i,y_j)$ along a constant value of y are shown in Fig. 7a. $S_B(x_i,y_j)$ was known from previous measurements of the signal caused by the beam in the absence of a sample. By carrying out the signal transfer analysis, the moisture profiles at the times of the measurements were calculated and are displayed in Fig. 7b. From this data on the moisture distribution, the moisture transfer coefficient of the sample material was determined.

4.2. Numerical analysis

The best moisture transfer coefficient obtained from the experimental profiles combined with the numerical procedure outlined in section 3.2. is given in Fig. 8. This transfer coefficient takes into account molecular diffusion and capillary pressure mechanisms. At high moisture content, the transfer coefficient increases rapidly and the moisture motion is predominantly governed by capillary pressure. At low moisture content, molecular diffusion can be considered the main transfer mechanism [22]. In Fig. 9 the comparison between experimental and calculated moisture profiles is given for t = 1, 2, 7, 14 and 21 days of drying time (dashed lines: experimental, solid lines: numerical simulation).

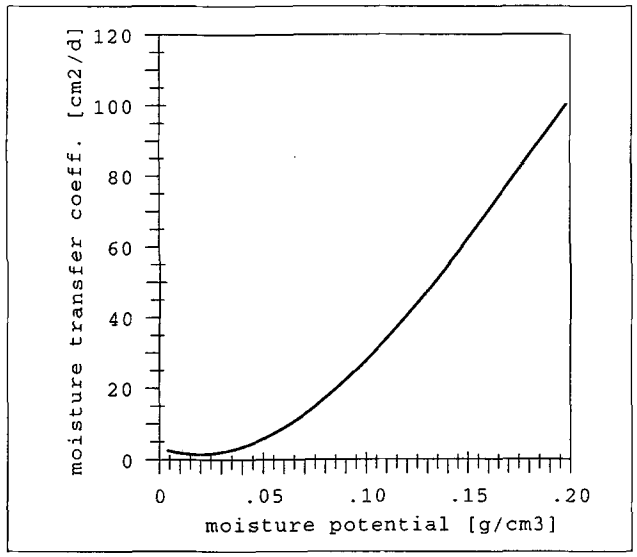

Fig. 8 – Moisture transfer coefficient as a function of moisture potential.

5. CONCLUSION

The presented technique constitutes a new experimental/analytical tool for the determination of moisture distributions in porous building materials. By formulating the process in terms of system transfer functions it provides a simple and efficient procedure for the interpretation of the complex transmission process. It profits from the high moisture detection sensitivity which is

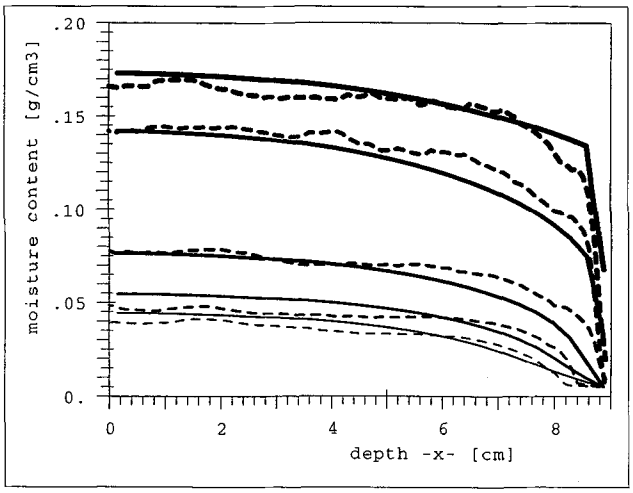

Fig. 9 – Moisture profiles in the drying specimen after 1, 2, 7, 14 and 21 days. Comparison between experiments (dashed curves) and numerical simulation (solid curves).

physically inherent in a neutronic method, and also offers good spatial resolution. The experimental data can be used for validation of transport models and for the determination of the parameters of the transfer coefficient. Combined with numerical analysis the method can be applied to the study of various mechanisms of moisture transport in porous building materials and it can also be employed as a complementary technique in combination with other methods.

ACKNOWLEDGMENTS

The authors would like to thank H. Böck of the Atominstitute of the Austrian Universities for his essential support to the experimental work, E. Lehmann of the Paul Scherrer Institute for his advice, S. Körner of the Atominstitute of the Austrian Universities for her contribution to the Monte Carlo calculations and for her help with the experimental work, K. Helbling and T. Jaggi of the Swiss Federal Institute of Technology for the preparation of the samples, A. Gerdes of the Swiss Federal Institute of Technology for his help and advice concerning the chemical analysis of the samples and S. Engel of the Swiss Defense Technology and Procurement Agency for his help in optimizing the process of digitization of the images.

REFERENCES

[1] Pel, L., Kopinga, K., Bertram, G. and Lang, G., 'Water absorption in fired-clay brick observed by NMR-scanning', *J.Phys.D.: Appl.Phys* **4** (1995) 675-680.

[2] Queisser, A., 'Zerstörungsfreie Materialuntersuchungen an Natursandstein mittels Computer Tomographie', *Bautenschutz und Bausanierung* **11** (1988) 54-60.

[3] Quenard, D. and Sallee, H., 'A gamma-ray spectrometer for measurement of the water diffusitivity of cementitious materials', Mat. Res.Soc. Symp. Proc. 137 (1989), 165-169.

[4] Peterka, F., Böck, H., Pleinert, H. and Slonc, T, 'Instrumental neutron transmission analysis technique of building material', in 'Neutron Radiography (4)', Proceedings of the Fourth World Conference on Neutron Radiography, San Francisco, 1992 (Kluwer, Dordrecht, 1993) 83-93.

[5] Pel, L., Ketelaars, A.A., Adan, O.C.G. and van Well, A.A., 'Determination of moisture diffusitivity in porous media using scanning neutron radiography', *Int. J. Heat Mass Transfer* **36** (1993) 1261-1267.

[6] Domanus, J.C., Matfield, R., Markgraf, J.F.W. and D.J. Taylor, 'Imaging techniques', in 'Practical Neutron Radiography' (Kluwer, Dordrecht, 1992) 51-56.

[7] Wyman, D.R. and Harms, A.A., 'System transfer function applications in neutron radiographic object scattering', *Nuclear Science and Engineering* **88** (1984) 522-536.

[8] Segal, Y., Gutmann, A., Fishman, A., and Notea, A., 'Point spread functions due to neutron scattering in thermal neutron radiography of aluminium, iron, zirkaloy and polyethylene objects', *Nuclear Instruments and Methods* **197** (1982) 557-562.

[9] Pleinert, H. and Lehmann, E., 'Quantitative neutron radiography measurement of hydrogenous distribution' in 'Neutron Radiography (5)', Proceedings of the Fifth World Conference on Neutron Radiography, Berlin, June, 1996.

[10] Greim, L., Leeflang, H.P. and Matfield, R., 'Neutron Sources', in 'Practical Neutron Radiography' (Kluwer, Dordrecht, 1992) 12-25.

[11] Lehmann, E., Pleinert, H. and Wiezel, L., 'Design of a neutron radiography facility at the Spallation neutron source SINQ', *Nuclear Instruments and Methods* **A 377** (1996) 11-15.

[12] Domanus, J.C. and Greim, L., 'Collimators', in 'Practical Neutron Radiography' (Kluwer, Dordrecht, 1992) 96-126.

[13] Markgraf, J.W. and Matfiel, R, 'Converters', in *Ibid.* 77-87.

[14] Kobayashi, H., Tomura, K., Harasawa, S. and Hattori, M., 'Neutron radiography using cooled CCD-Camera', in 'Neutron Radiography (3)', Proceedings of the Third World Conference on Neutron Radiography, Osaka, May, 1989 (Kluwer, Dordrecht, 1990) 421-428.

[15] Takashi, K., Tazaki, S., Miyahara, J., Karasawa, Y. and Niimura, N., 'Imaging performance of imaging plate neutron detectors', *Nuclear Instruments and Methods* **A 377** (1996) 119-122.

[16] Ashoub, N., Böck, H. and Scherpke, G., 'The Neutron Radiography Facility at the Atominstitut-Vienna', in 'Nuclear Energy in Central Europe - Present and Perspectives', Proceedings of the Regional Meeting, Portoroz, June 1993, 602-609.

[17] Peterka, F. and Slonc, T, 'Quantitative neutron transmission analysis experimental method using film as neutron detector', in 'Neutron Radiography (3)', Proceedings of the Third World Conference on Neutron Radiography, Osaka, 1989 (Kluwer, Dordrecht, 1990) 331-340.

[18] Harms, A.A. and Wyman, D.R., 'Mathematics and Physics of Neutron Radiography' (D.Reidel, Dordrecht, 1986).

[19] Körner, S., private communication, 1997.

[20] Cashwell, E.D. and Everett, C.J, 'Monte Carlo Method for Random Walk Problems' (Pergamon Press, New York, 1959).

[21] Briesmeister, J.F., 'MCNP - a General Monte Carlo n-Particle Transport Code, Version 4A' (Los Alamos Rep. LA-12625-M, 1993).

[22] Garrecht, H., 'Porenstrukturmodelle für den Feuchtehaushalt von Baustoffen mit und ohne Salzbefrachtung und rechnerische Anwendung auf Mauerwerk', PhD thesis, Universität Fridericana zu Karlsruhe, Germany, 1992.

[23] Mayer, G. and Wittmann, F.H., 'Ein Modell zur Beschreibung des Wasser- und Salztransportes in Mauerwerk', *Int. Zeitschrift für Bauinstandsetzen*, 2. Jahrgang, Heft **1** (1996) 67-82.

[24] Mayer, G., 'Feuchte- und Salztransport in porösen Werkstoffen des Bauwesens', PhD thesis, ETH-Zürich, 1997.

[25] Weimann, M., private communication, 1997.

[26] Narasimhan, T.N. and Witherspoon, P.A., 'An integrated finite difference method for analyzing fluid flow in porous media', *Water Resources Research* (1989) 57-64.

[27] Wittmann, X., Sadouki, H. and Wittmann, F.H., 'Numerical evaluation of drying test data', Transaction 10th Int. Conf. on Struct. Mech. in Reactor Techn., Vol Q (1989) 71-79.